V-shaped inversion domains in InN grown on c-plane sapphire

J. Jasinski[a,b] and Z. Liliental-Weber

Lawrence Berkeley National Laboratory, Materials Science Division, 1 Cyclotron Rd., Berkeley, CA 94720

H. Lu and W. J. Schaff

Department of Electrical and Computer Engineering, Cornell University, Ithaca, NY 14853

Inversion domains with a V-shape were found to nucleate inside a Mg-doped InN heteroepitaxial layer. They resemble Al-polarity domains, observed recently, in N-polarity AlN films. However, the angle between the side-walls of the V-shaped domain and the c-axis differs in these two cases. In InN, this angle is almost two times bigger than that reported for AlN. The origin of V-shaped inversion domains in InN film is not yet clear.

[a] E-mail: jbjasinski@lbl.gov
[b] current address: University of California, Merced, CA 95344

In recent years, there has been a rapid development of nitride based electronic and optoelectronic devices, such as blue and ultraviolet diodes, lasers and photodetectors, as well as transistors and high power devices. Due to the lack of large native substrates, most such devices are grown heteroepitaxily on foreign substrates. A number of different substrates have been proposed and c-plane sapphire or 6H SiC are the most commonly used among them. Growth on a foreign substrate leads, however, to a high density of structural defects. A lattice mismatch and a difference in thermal expansion coefficient result in threading dislocations at densities typically in the range of 10^9 – 10^{10} cm^{-2}. Although threading dislocations are dominant structural defects in nitride layers, other defects can also be formed under specific growth conditions. These include the use of a non-conventional substrate or substrate orientation, heavy doping, or a rough substrate surface. For example, it is known that the growth of m-plane GaN on $LiAlO_2$ [1-3], or the growth of a-plane nitrides on r-plane sapphire [4,5], leads to a high density of low-energy basal stacking faults. Another example consists of pyramidal defects, which are formed when GaN [6-8] or AlGaN [9] is heavily doped with Mg. There are also some experimental results suggesting that heavy Si doping of GaN leads to the formation of clusters of point defects [10]. Another example of impurity-related structural defects are oxygen-rich nanopipes, decorating screw dislocations, in GaN layers grown by hydride vapor phase epitaxy (HVPE) [11].

Important and common structural defects in nitride layers are also inversion domains (IDs), which can be understood as follows. All III-V nitrides, when grown on a c-plane sapphire substrate, crystallize in the stable wurtzite phase structure. However, for growth along the c-axis, atomic bonds can have one of two opposite orientations. As a

result, layers with two opposite growth polarities can be produced. The layer grown with N-polarity has the bond parallel to the c-axis oriented in such a way that the growth direction points from the N atom towards the group III metal atom. The growth with metal-polarity corresponds to the opposite bond orientation. An inversion domain has opposite growth polarity compared to that of the matrix.

Inversion domains have been extensively studied in the case of GaN layers [12-17]. In fact, several types of IDs have been reported for this material. The two most commonly observed are: (1) “house”- shaped domains formed in GaN films grown either by metal-organic chemical vapor deposition [12,13] or by HVPE [14] and, (2) long, narrow domains, in the form of hexagonal columns which nucleate in the GaN layers, grown by molecular beam epitaxy (MBE) [14-16]. Also, as previously mentioned, pyramidal, hexagonal defects that are observed in heavily Mg-doped GaN samples are believed to be IDs [18,19]. Unlike in the case of GaN, there are only a very few reports of IDs in heteroepitaxial AlN layers [20,21] and no reports so far on such defects in the InN layers. Interestingly, columnar IDs observed in AlN films grown on sapphire differ from such domains in GaN films. In AlN layers, these domains nucleate at the layer/substrate interface as very narrow columns, but then, unlike in the case of GaN, they widen at a steady rate when growth proceeds. As a result, domains with a V-like shape are formed [20]. The density of these domains can be controlled by the growth conditions [22]. Here, we report formation of similar V-like IDs in InN films grown on c-plane sapphire. The structural properties of these domains will be discussed, and experimental evidence will be provided to support their identification.

The InN layer studied here was grown on (0001)-oriented (c-plane) sapphire substrates using conventional MBE system. The details of this growth procedure have been described elsewhere [23]. The buffer layer used was a 220 nm-thick GaN layer grown on 10 nm-thick AlN nucleation layer. The thickness of the InN film was 0.5 μm. This film was grown at 550 ^{o}C at a rate of 12 nm/min. The growth temperatures for AlN and GaN were 850 ^{o}C and 820 ^{o}C, respectively. The InN layer was doped with Mg to obtain p-doping. However, this was not achieved and the layer had n-type electrical conductivity. The concentration and mobility, estimated based on Hall effect measurements, were ~1x10^{18} cm^{-3} and 100 cm^{2}/Vs, respectively. The sample was studied using a JEOL JEM3010 transmission electron microscope (TEM), operated at 300 kV. Cross-sectional TEM specimens were prepared by the standard method of mechanical pre-thinning followed by Ar-ion milling.

A typical TEM micrograph of the layer structure observed along the [11$\underline{2}$0] projection is shown in Fig. 1a. This is a bright field micrograph, taken under two beam conditions, with a diffraction vector parallel to the c-axis. It can be noticed that, in addition to threading dislocations, the InN layer contains V-like defects (indicated by arrows) with an estimated density on the order of 10^{9} cm^{-2}. Interestingly, all these defects nucleated a few tens of nanometers (usually 40-60 nm) above the InN/GaN interface and then propagated through the entire layer, to its surface. Fig. 1b shows a bright-field TEM micrograph of the same layer, but observed along the [1$\underline{1}$00] projection. Here, again, the defects with V-shape are visible with similar density. Fig. 1c shows a higher magnification bright field micrograph of such a V-shaped defect.

Diffraction contrast experiments indicate that boundaries of V-defects are in strong contrast for the **g**-vector parallel to the c-axis (Fig.2a) and are out of contrast for the **g**-vector perpendicular to the c-axis (Fig. 2b). This suggests that there is a displacement along the c-axis at these boundaries similar to what has been reported for IDs in GaN [12] and AlN [20] films.

In order to prove that V-defects in InN are IDs we used the criterion proposed by Serneels et al. [24]. Under multiple diffraction conditions we collected pairs of dark field micrographs of the same V-like defect. The first micrograph the pair was recorded for a **g**-vector equal to (000$\underline{2}$) and the second one for the opposite **g**–vector. The pair of micrographs is shown in Fig. 3. A defect-matrix contrast reversal can be noticed between these two micrographs, despite a strong overall contrast variation due to the change in specimen thickness. In the micrograph shown in Fig. 3a, the upper part of the V-shaped defect is brighter than the matrix. Further from the surface it becomes darker than the matrix and then again brighter. The reversed sequence can be seen in the micrograph shown in Fig. 3b, which according to the criterion from the Ref. 24, proves that the V-like defects are IDs.

V-shaped IDs in our InN film often emerge at the surface, in the middle of an island, and their tips stick out above the surface (see Fig. 1c). This indicates that the growth rate of the material inside IDs is higher than that of the matrix. A similar behavior has been observed in the case of IDs grown with metal-polarity inside N-polarity AlN [20] or GaN [15] films. Therefore, it may suggest that V-like IDs in our InN film were also grown with metal-polarity (i.e. In-polarity) and are embedded in a material grown with N-polarity.

Despite many similarities between V-like IDs in our InN film and these observed in AlN films, there are also some differences between these two cases. First of all, the divergence angle between two opposite arms of these domains in InN is approximately 8^o, whereas for AlN films it is about 4.5^o [20]. The origin of this difference is not yet clear. The second difference between the two cases relates to the region where IDs nucleate. In AlN films, the domains have been observed to nucleate directly at the substrate surface [20], whereas here, in InN, they typically nucleated inside the layer, at approximately the same distance above the interface with GaN. This may suggest that, during the growth of InN, some impurities were accumulating at the growth surface and caused the nucleation of IDs. Mg doping could be suspected; however, we did not observe such IDs in another Mg-doped InN layer. We also did not observe such domains in undoped InN layers. Therefore, it is possible that a complex of Mg and some other impurity may be responsible for the nucleation of V-shaped IDs in InN films.

In conclusion, TEM studies were used to identify V-shaped inversion domains in a Mg-doped MBE-grown InN film. These domains were grown at a higher growth rate than the layer. They are similar to domains reported recently for AlN films; however, there are some substantial differences between these two cases.

Work at LBNL was supported by the Director, Office of Science, Office of Basic Energy Science of the U.S. Department of Energy under Contract No. DE-AC03-76SF00098. The Cornell MBE growths were supported by LBNL subcontract 6703656. The TEM group (J.J. and Z.L.-W.) would like to thank the National Center for Electron Microscopy at LBNL for the opportunity to use its facilities.

References

1. Y. J. Sun, O. Brandt, U. Jahn, T. Y. Liu, A. Trampert, S. Cronenberg, S. Dhar, and K. H. Ploog, J. Appl. Phys. **92**, 5714 (2002).
2. J. Jasinski, Z. Liliental-Weber, H. P. Maruska, B. H. Chai, D. W. Hill, M. M. C. Chou, J. J. Gallagher, S. Brown, Mat. Res. Soc. Symp. Proc. **764**, C6.6.1 (2003).
3. R. R. Vanfleet, J. A. Simmons, H. P. Maruska, D. W. Hill, M. M. C. Chou, and B. H. Chai, Appl. Phys. Lett. **83**, 1139 (2003).
4. M. D. Craven, S. H. Lim, F. Wu, J. S. Speck, and S. P. DenBaars, Appl. Phys. Lett. **81**, 469 (2002).
5. K. Dovidenko, S. Oktyabrsky, and J. Narayan, J. Appl. Phys. **82**, 4296 (1997).
6. Z. Liliental-Weber, M. Benamara, J. Washburn, I. Grzegory, and S. Porowski, Phys. Rev. Lett. **83**, 2370 (1999).
7. Z. Liliental-Weber, M. Benamara, W. Swider, J. Washburn, I. Grzegory, S. Porowski, D. J. H. Lambert, C. J. Eiting, and R. D. Dupuis, Appl. Phys. Lett. **75**, 4159 (1999).
8. P. Vennéguès, M. Benaissa, B. Beaumont, E. Feltin, P. De Mierry, S. Dalmasso, M. Leroux, and P. Gibart, Appl. Phys. Lett. **77**, 880 (2000).
9. M. Hansen, L. F. Chen, S. H. Lim, S. P. DenBaars, and J. S. Speck, Appl. Phys. Lett. **80**, 2469 (2002).
10. Z. Liliental-Weber, D. Zakharov, J. Jasinski, unpublished data.
11. Z. Liliental-Weber, J. Jasinski, J. Washburn and M.A. O'Keefe, Microscopy and Microanalysis **8**, 1198 (2002).
12. X. H. Wu, L. M. Brown, D. Kapolnek, S. Keller, B. Keller, S. P. DenBaars, and J. S. Speck, J. Appl. Phys. **80**, 3228 (1996).

13. L. Romano, J. Northrup, and M. O'Keefe, Appl. Phys. Lett. **69**, 2394 (1996).

14. V. Potin, P. Ruterana, and G. Nouet, J. Appl. Phys. **82**, 2176 (1997).

15. V. Potin, , P. Ruterana and G. Nouet, Mater. Sci. & Eng. B **59**, 173 (1999).

16. H. Zhou, F. Phillipp, M. Gross, H. Schroder, Mater. Sci. & Eng. B **68**, 26 (1999).

17. D. Cherns D, W. T. Young, F. A. Ponce, Mater. Sci. & Eng. B **50**, 76 (1997).

18. P. Vennéguès, M. Benaissa, S. Dalmasso, M. Leroux, E. Feltin, P. De Mierry, B. Beaumont, B. Damilano, N. Grandjean and P. Gibart, Mater. Sci & Eng. B **93**, 224 (2002).

19. Z. Liliental-Weber, T. Tomaszewicz, D. Zakharov, J. Jasinski, M.A. O'Keefe, S. Hautakangas, A. Laakso, and K. Saarinen, Mat. Res. Soc. Symp. Proc. **798**, Y9.7.1 (2004).

20. J. Jasinski, Z. Liliental-Weber, Q. S. Paduano, D. W. Weyburne, Appl. Phys. Lett. **83**, 2811 (2003).

21. J. Jasinski, T. Tomaszewicz, Z. Liliental-Weber, Q. S. Paduano, D. W. Weyburne, Mat. Res. Soc. Symp. Proc. **798**, Y5.29.1 (2004).

22. Q.S. Paduano, D.W. Weyburne, J. Jasinski, and Z. Liliental-Weber, J. Cryst. Growth **261**, 259 (2004).

23. H. Lu, W. J. Schaff, J. Hwang, H. Wu, W. Yeo, A. Pharkya, and L. F. Eastman, Appl. Phys. Lett. **77**, 2548 (2000).

24. R. Serneels, M. Snykers, P. Delavignette, R. Gevers, and S. Amelinckx, Phys. Status Solidi B **58**, 277 (1973).

Figure Captions

Fig. 1. (a), (b) Two-beam bright-filed TEM micrographs of the InN film observed in cross-section along the [11$\underline{2}$0] and [1$\underline{1}$00] directions, respectively. V-shaped domains are indicated by small arrows. (c) A singe domain shown at higher magnification.

Fig. 2. Two-beam dark-field TEM micrographs of the InN layer. These micrographs were recorded with the **g**-vector equal to (0002) and (1120), respectively.

Fig. 3. Two-beam dark-field TEM micrographs of an inversion domain in the InN film. These micrographs were recorded with the **g**-vector equal to (0002) and (000$\underline{2}$), respectively. A domain-matrix contrast reversal can be noticed.

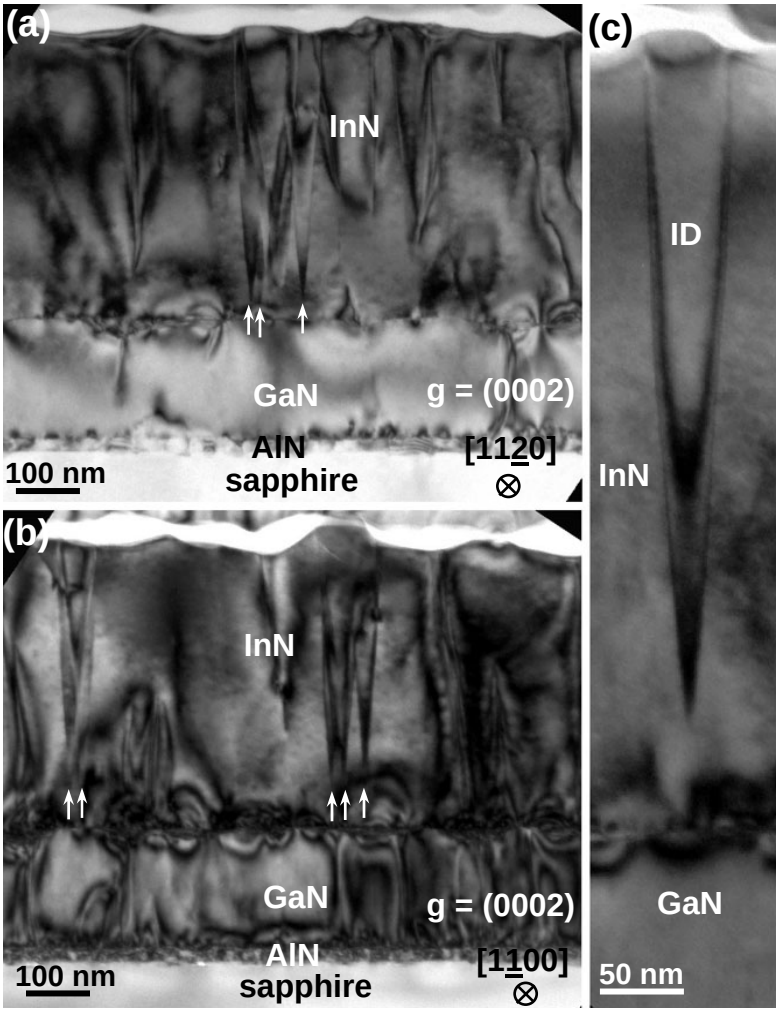

Fig. 1
(*J. Jasinski, et al. "V-shaped inversion domains in InN grown on c-plane sapphire")*

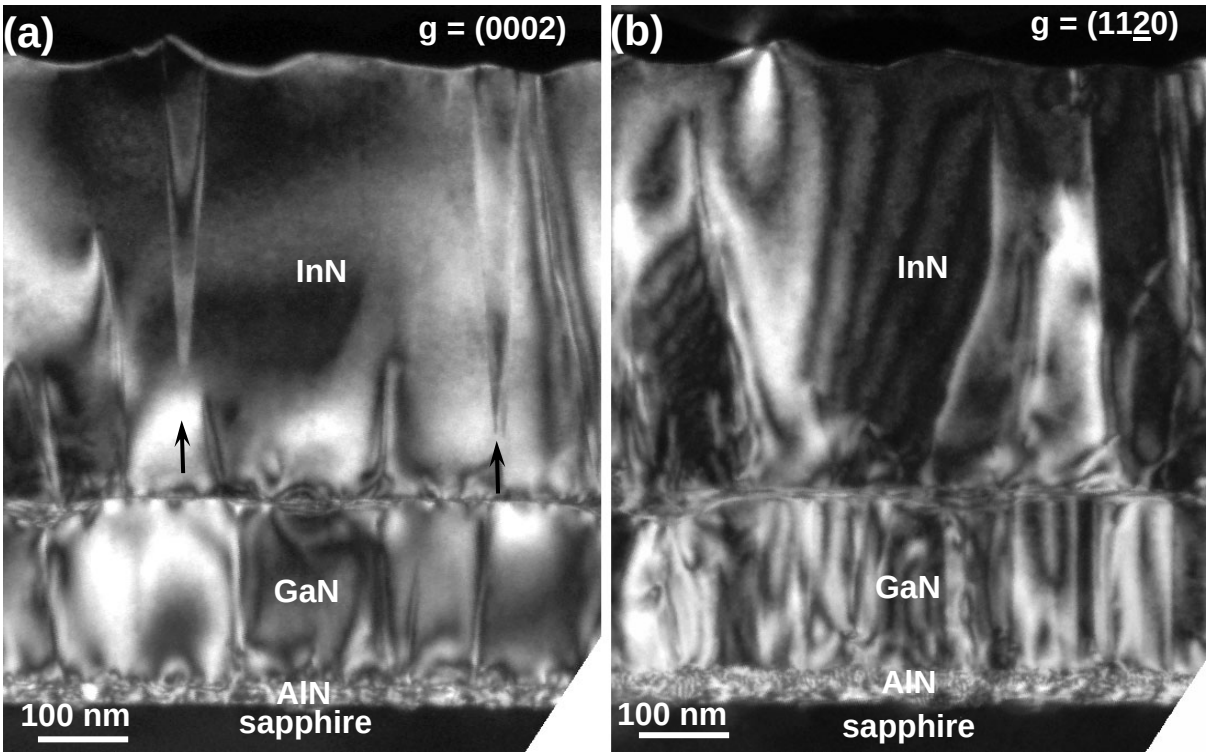

Fig. 2
(*J. Jasinski, et al. "V-shaped inversion domains in InN grown on c-plane sapphire")*

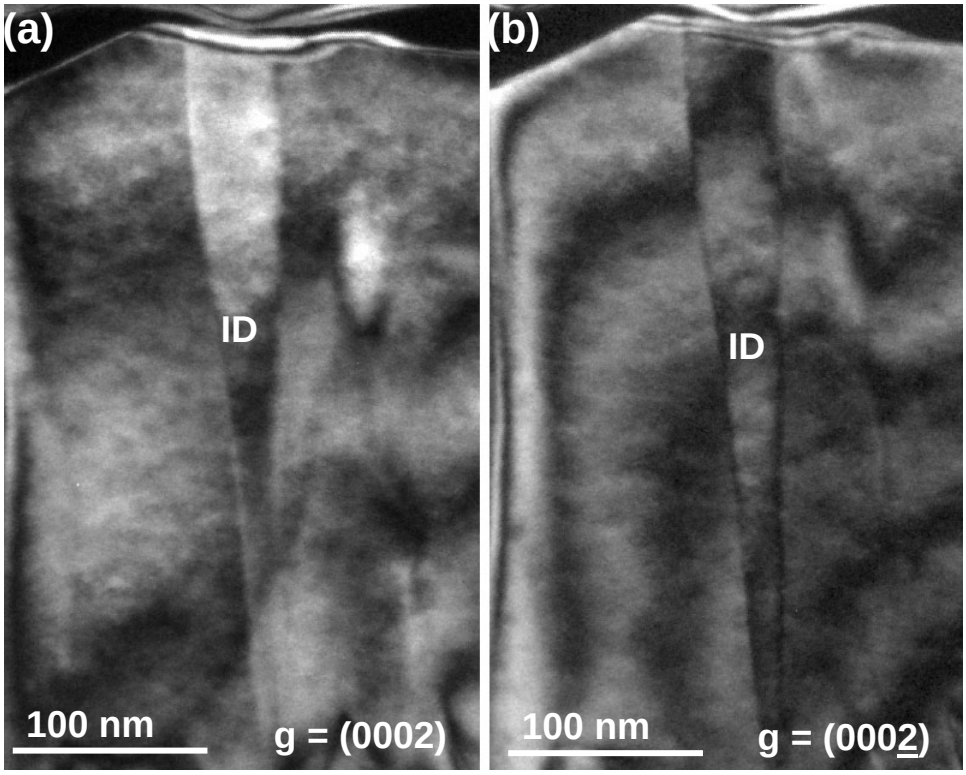

Fig. 3
(*J. Jasinski, et al. "V-shaped inversion domains in InN grown on c-plane sapphire")*